Heat island influence on space-conditioning loads of urban and suburban office buildings

K. R. Gunawardena[1], N. McCullen[1], and T. Kershaw[1]

[1] Department of Architecture and Civil Engineering, University of Bath,
Claverton Down, Bath, BA2 7AY, UK
t.j.kershaw@bath.ac.uk

Abstract. A warming climate, increasing frequency and severity of extreme heat events, and the urban heat island (UHI) effect are cumulatively expected to exacerbate thermal loading on buildings. This paper examines how the UHI affects space-conditioning loads within urban and suburban office buildings, and how the trend of replacing traditional heavyweight facades with lightweight alternatives affect both the magnitude and timing of the UHI and resulting building energy use. The paper addresses this through simulation studies of typical street canyons based on the urban Moorgate and suburban Wimbledon areas of London. Results show that including the UHI within a dynamic thermal simulation has an adverse effect on urban annual space-conditioning, with a 4 % increase in demand for buildings with stone facades, while a glazed alternative show a 10 % increase. For the corresponding effect on suburban annual space-conditioning, a modest 1.2 % decrease for buildings with brick facades is shown, while the alternative white painted timber construction shows a marginal 0.8 % increase. The study demonstrates that the trend in urban centres to replace heavyweight facades with lightweight insulated ones would increase space-conditioning loads by 2.3 %, and therefore adversely affect the UHI to create a vicious cycle of additional urban warming. Within a suburban context however, changing from heavyweight to lightweight insulated facades decreased space-conditioning loads by 5 % to provide a beneficial effect. The study in turn stresses the significance of accounting for UHI loads in estimating urban and suburban energy use, for which a combined simulation approach has been presented as a practical pathway.

Keywords: Heat island impact, space-conditioning loads, urban energy use.

1 Introduction

The predictions of increasing frequency and severity of extreme heat events from climate change are a significant challenge to the global trend towards urbanisation [1]. The situation is made more complex in cities by the long-established warming induced by the urban heat island (UHI) effect [2, 3]. Such enhanced climatic loads can exert significant influence on the sustainable operation of urban settlements. Understanding the interactions between the built-environment and its dynamic climate is therefore necessary for delivering sustainable urban growth.

Central to understanding urban climate interactions is the 'urban energy balance' that represents the partitioning of incoming and outgoing energy flows of the urban surface system [4]. The typically warmer climate experienced in cities is explained by the net positive thermal balance that leads to the formation of UHIs. This net positive thermal balance arises from changes to their surface properties that include increased surface roughness, reduced albedo, reduced green and blue space for evaporation, and increased anthropogenic heat generated from human activities. The resulting UHI effect can be considered as an added environmental thermal load that affects how energy is used within buildings [5]. This energy use within buildings in turn contributes heat to the UHI as anthropogenic emissions. Higher building energy usage could therefore contribute to the storage of greater thermal energy in the urban system and thereby help generate and intensify UHIs [3]. This suggests that if high-energy solutions are used to condition buildings, a vicious cycle of warming may result to create an ever worsening and unhealthy urban environment. This is made more complicated by modern construction practices following a trend towards replacing traditional heavyweight facades with lightweight and insulated alternatives.

The purpose of this study is to identify heat island influence and its degree of significance to urban and suburban office building space-conditioning loads. This will be examined through the comparison of dominant 'heavyweight' and 'lightweight' construction build-ups situated within the morphological contexts of central urban and suburban areas. The method for addressing this considers simulations of idealised street canyons, based on the morphologies of the Moorgate (central urban) and Wimbledon (suburban) areas of London. To achieve this in a manner suitable for wider applicability, the study presents a combined approach of using a multiscale coupled urban climate model and a building energy model as a practical simulation pathway.

1.1 Characterising the urban climate

Sourcing measurement data from direct techniques (using eddy flux stations with anemometers, thermocouples, gas analysers etc.) to compile localised weather profiles offers the most accurate means to account for site-specific climate loading. For these measurements to be representative however, the data would require longitudinal measurement to account for the spatial and temporal diversity of UHI influence [3]. This requirement would favour data collection methodologies utilising dense networks of fixed sites as opposed to mobile traverse observations that offer only cross-sectional data. There is however no general scheme or accepted standard practice to direct such measurement gathering practices currently in place in cities [5]. This means that proposed studies would have to setup their own infrastructure to gather data. Even though such measurement based studies exist [e.g. 6, 7, 8], the infrastructural cost required to achieve similar programs of data collection are unlikely to be available for all studies [9]. Data collected from private networks and enthusiasts may be considered as an alternative. This data however is likely to be unreliable, with limited parameters collected and data showing gaps that require laborious interpolation methods to complete.

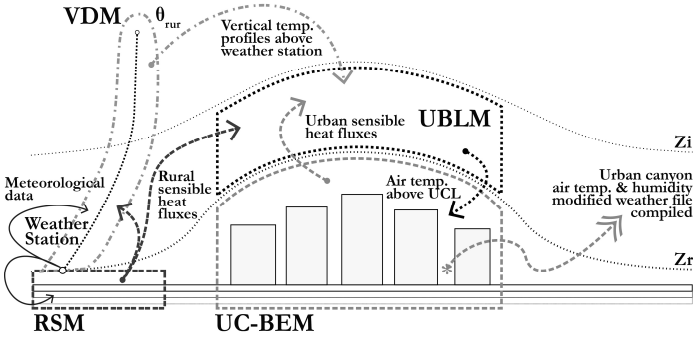

Fig. 1. The physical domain of the UWG modules and their data exchanges within an ideal city, based on Bueno, Norford [10].

To overcome the many challenges of accounting for the complexities of the interrelated urban climate, this study uses a modified version [5.1.0 beta, 11] of the multiscale coupled framework termed the 'Urban Weather Generator' (UWG) [12]. The UWG presented schematically in Fig. 1, is based on Monin-Obukhov similarity theory and is composed of four coupled sub-models that include a Rural Station Model (RSM), Vertical Diffusion Model (VDM), Urban Boundary Layer Model (UBLM), and an Urban Canopy and Building Energy Model (UC-BEM) based on the Masson [13] Town Energy Balance scheme and a building energy model developed by Bueno, Norford [14]. These sub-models exchange data to calculate modified temperature and humidity values and compile a modified weather file in the EnergyPlus (.epw) format for use by dynamic building thermal modelling software. A summary of the basic data exchanges involved is presented in Fig. 1, while detailed descriptions are offered in Bueno, Norford [10], [15]. The UWG has been verified against field data from Basel, Toulouse, and Singapore [10, 15, 16]. The verifications from Basel and Toulouse demonstrated that urban climate estimation requires both canopy and boundary layer effects in order to account for the aggregated influence of the UHI over the entire city; with more than half the influence observed in urban canyons attributed to the mesoscale effect. The resolution of such boundary layer influences require mesoscale processes to be reconciled with the aid of higher-scale atmospheric simulations coupled within a framework as employed by the UWG [10].

Fig. 2. Typical 'central urban' street canyon view of Moorgate (left); and 'suburban' street canyon view of Wimbledon, London (right); from ©Google Street-view.

2 Method

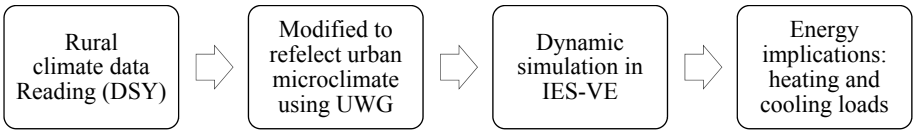

Fig. 3. Method pathway for study.

In this study, the morphology of the Moorgate and Wimbledon neighbourhoods of London are idealised by averaging their parameters to produce roughness profiles with a characteristic radius of 500 m. In all scenarios, the target canyon buildings have the same occupational profile of a medium-sized office building, and only differ between scenarios in terms of their façade construction as detailed in Appendix: Table 2. These profiles, together with a rural weather file (in .epw format) are then input into the UWG (5.1.0 beta) to generate weather profiles that include UHI influence on air temperature and humidity values for the canyon scenarios considered (see Table 1). The rural weather data used for this study is the Design Summer Year (DSY) for the Reading area (~60 km and ~52 km due west of the Moorgate and Wimbledon sites respectively), which was generated using the UKCP09 Weather Generator, the full methodology of which is described in Eames, Kershaw [17]. This input weather data represents the rural boundary condition where the influence of the city is assumed as negligible. The Reading file was also selected for this study as it presented relatively clear (minimal cloud cover) conditions for both the summer and winter solstice days, which represents ideal conditions for UHI formation and serve as benchmark days to compare and assess the different heat island conditions generated. The resulting UWG profiles for the canyon scenarios were then applied to respective thermal models of the Moorgate and Wimbledon street canyons and their surrounding buildings, created in the dynamic simulation modelling package IES-VE [18] to estimate space-conditioning loads.

Table 1. Simulation scenarios.

	Weather file used	Constructions used
Urban		
Urb-Base Stone	Unmodified Design Summer Year (DSY) for Reading.	Using stone facades with glazing ratio (GR) of 0.30, detailed in Appendix: Table 2 (currently dominant among buildings of Moorgate).
Urb-Stone	The above modified using the UWG, i.e. with dominant construction of Stone facades and resulting UHI influence included.	
Urb-Base Glazed	Unmodified Design Summer Year (DSY) for Reading.	Using glazed facades with GR of 0.30, detailed in Appendix Table 3 (hypothetical).
Urb-Glazed	The above modified using the UWG, i.e. with dominant construction of Glazed facades and resulting UHI influence included.	

	Weather file used	Constructions used
Suburban		
SUrb-Base brick	Unmodified Design Summer Year (DSY) for Reading.	Using brick facades with GR of 0.30, detailed in Appendix: Table 2 (currently dominant among buildings of Wimbledon).
SUrb-Brick	The above modified using the UWG, i.e. with dominant construction of brick facades and resulting UHI effect included.	
SUrb-Base Timber	Unmodified Design Summer Year (DSY) for Reading.	White painted timber facades with GR of 0.30, detailed in Appendix: Table 3 (hypothetical).
SUrb-Timber	The above modified using the UWG, i.e. with dominant construction of white painted timber facades and resulting UHI effect included.	

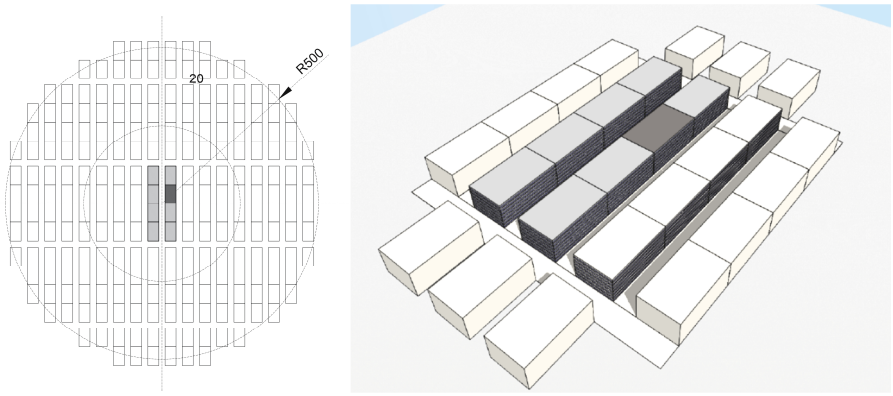

Fig. 4. Idealised radial area of the central urban condition (based on Moorgate) used for UWG microclimate generation (left), and its corresponding focused street canyon model used for IES-VE energy simulations (right).

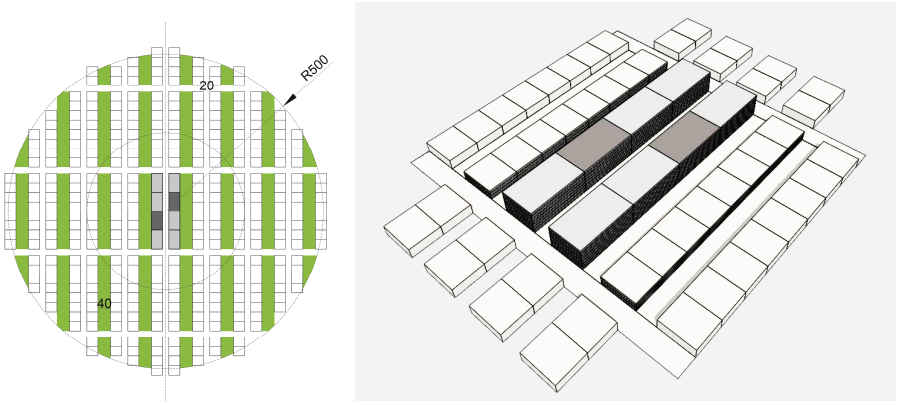

Fig. 5. Radial suburban condition (based on Wimbledon) used for UWG microclimate generation (left), and its corresponding street canyon model used for IES-VE energy simulations (right).

3 Results

The following presents firstly, the features of the weather files generated by the UWG with the UHI influence included; secondly, their resulting external building surface temperatures; and thirdly, their influence on internal space-conditioning loads for buildings that belong to the Moorgate (central urban) and Wimbledon (suburban) street canyons, highlighted in Fig. 4 and Fig. 5 respectively.

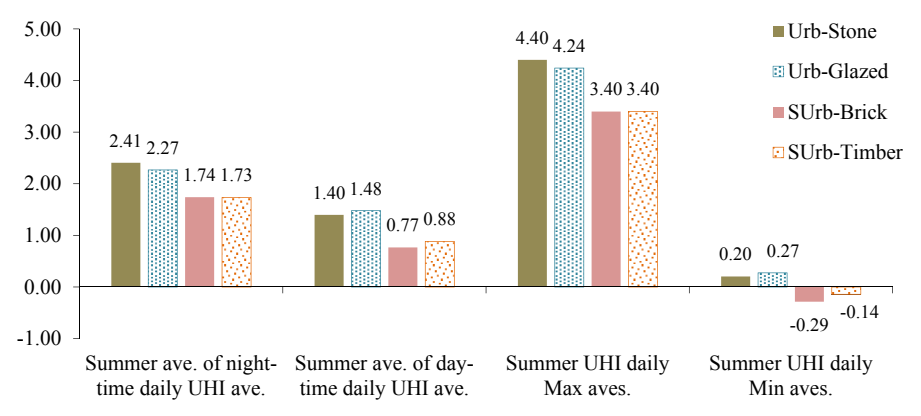

Fig. 6. Summertime (May-September) UHI features for scenarios simulated (K).

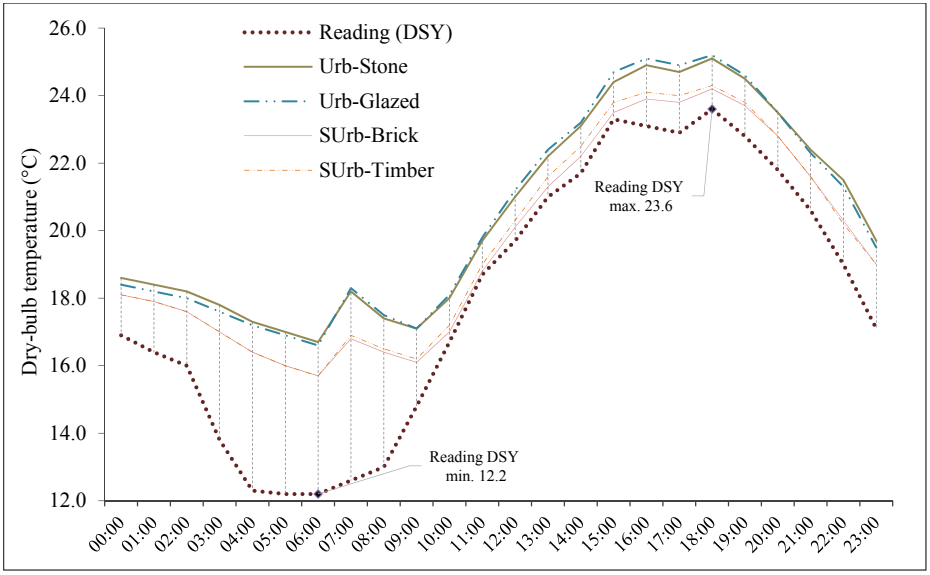

Fig. 7. Summer solstice (21-June) dry-bulb temperature profiles for Urb-Stone, Urb-Glazed, SUrb-Brick, and SUrb-Timber scenarios relative to the Reading (DSY) profile.

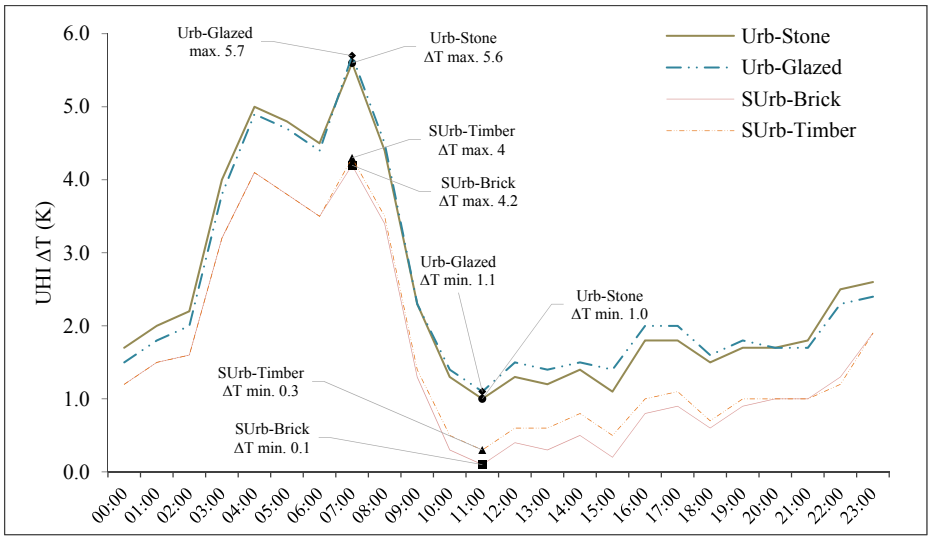

Fig. 8. Summer solstice (21-June) UHI ΔT (intensity) profiles (K) for Urb-Stone, Urb-Glazed, SUrb-Brick, and SUrb-Timber scenarios.

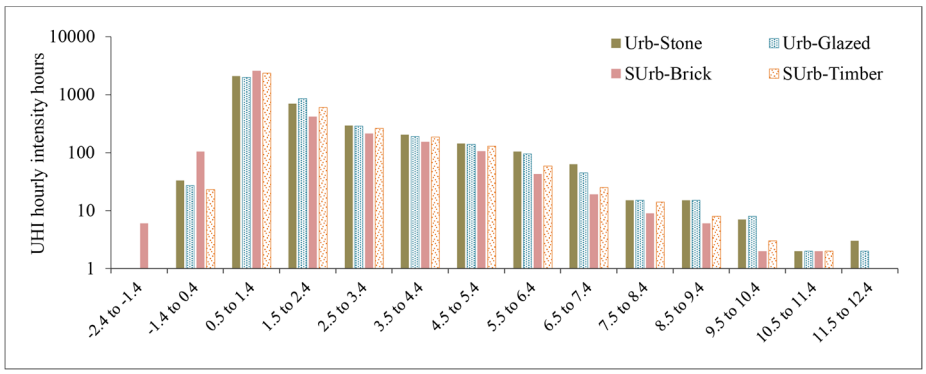

Fig. 9. Summer (May-September) urban & suburban UHI intensity (K) frequency Log10 (hrs).

3.1 Canyon microclimate profiles

The summer UHI average daily maximums for urban and suburban scenarios ranged from 3.40 to 4.40 K, while the average daily minimums ranged from -0.29 to 0.27 K (see Fig. 6). Notably, the latter average daily minimums for the urban scenarios showed positive values, while the suburban scenarios generated negative values (negative ΔT is indicative of a dominant cool island effect). When hourly UHI intensity resolution was examined, cool island conditions were identified in all scenarios with intensities ranging from <0 to -2 K representing between ~1.7 to 2.5 % for urban scenarios, while the suburban scenarios showed a significantly higher proportion between 5 to 7 % of the (3,672) hours simulated. This hourly UHI ΔT resolution also identified peak values

ranging from >6.4 to ≤12.4 K that represented between 2 to 3 % for the urban scenarios, while for suburban scenarios it was a notably lower proportion of ~1% of the total hours simulated (see Fig. 9). The urban Stone scenario showed the highest number of hours reaching these peak and minimum values (UHI ΔT max. ~3 %, and ΔT min. ~2.5 %) relative to the Glazed scenario, while the suburban Brick scenario showed the highest number of hours reaching peak values (ΔT max. ~7 %) relative to Timber (although only a marginal relative deference was evident between ΔT min. values). When hours of the day were divided to daytime (12 hours from 6 AM to 6 PM) and night-time (the residual) urban and suburban UHI intensity averages, the daily daytime value ranged from 0.77 to 1.48 K, and the night-time ranged from 1.74 to 2.41 K. Across all scenarios the night-time averages were consistently higher than daytime values. However when comparing urban and suburban scenarios across all hours of the day, a marked drop in average intensity values were evident for the latter relative to the former (see Fig. 6).

While the above observations can be made for average values, examining daily profiles present deviations. The profiles for the summer solstice (21-June) illustrate an example (see Fig. 7 and Fig. 8) where the hourly UHI ΔT maximum for the day were reached in the morning at around 7 AM (more pronounced with urban than suburban), almost two hours after sunrise (around 4:50 AM). These summer solstice profiles also illustrate an example where the night-time temperatures are higher for the urban Stone scenario relative to its lightweight Glazed variation, while the converse was true during the midday to evening period of the day. For the corresponding suburban scenarios, the lightweight Timber scenario showed higher temperatures for the midday to evening period relative to Brick, although a nocturnal difference was not evident. What is clear from the comparison is that the urban scenario UHI ΔT profiles are considerably higher in magnitude (i.e. warmer) than corresponding suburban profiles (see Fig. 8).

3.2 External building surface temperatures

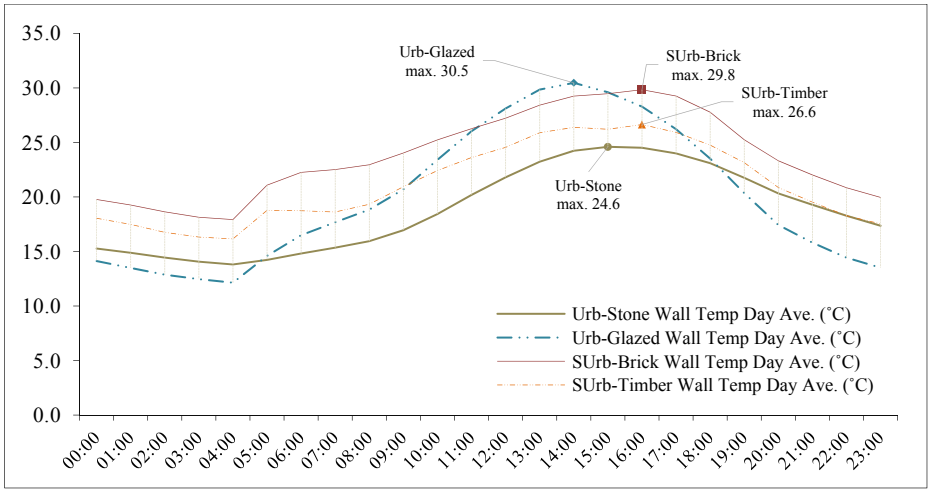

Fig. 10. Summer solstice (21-June) building external wall surface temperatures (˚C).

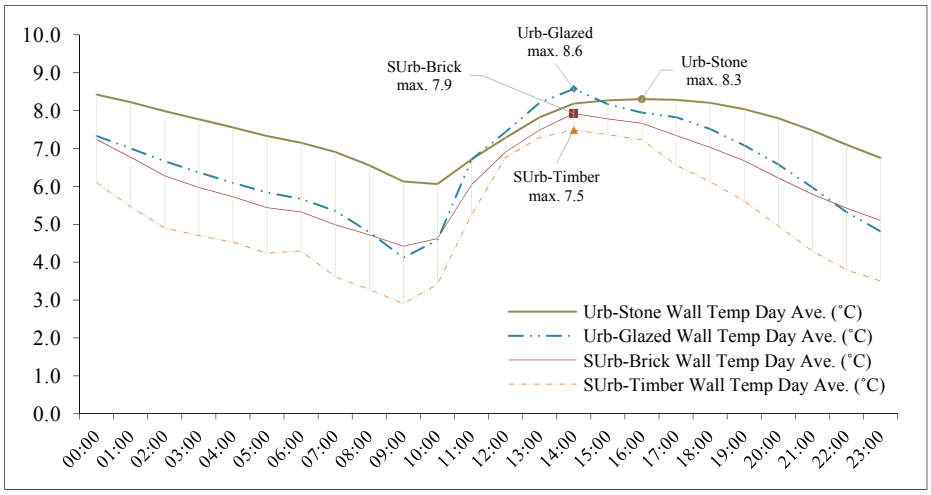

Fig. 11. Winter solstice (21-December) building external wall surface temperatures (˚C).

When annual external surface temperature averages were considered for urban scenarios, Stone surfaces were marginally warmer (13.9 ˚C) relative to Glazed (13.8 ˚C) surfaces. However as the above profiles show for both the summer and winter solstice (see Fig. 10 and Fig. 11), the peak surface temperature is higher for lightweight Glazed surfaces relative to heavyweight Stone. The corresponding annual surface temperature averages for the suburban scenario of Brick showed a significantly higher value (13.7 ˚C) relative to Timber (12.2 ˚C). However with the summer and winter solstice profiles, the peak temperatures for lightweight Timber surfaces remained considerably lower than the heavyweight Brick. The solstice profiles also showed a clear phase shift in peak temperatures for the urban Stone scenario relative to Glazed, with one hour for the summer and two for the winter (see Fig. 10). However for the corresponding suburban Brick and Timber scenarios, a similar phase shift was not evident (see Fig. 11).

3.3 Space-conditioning loads

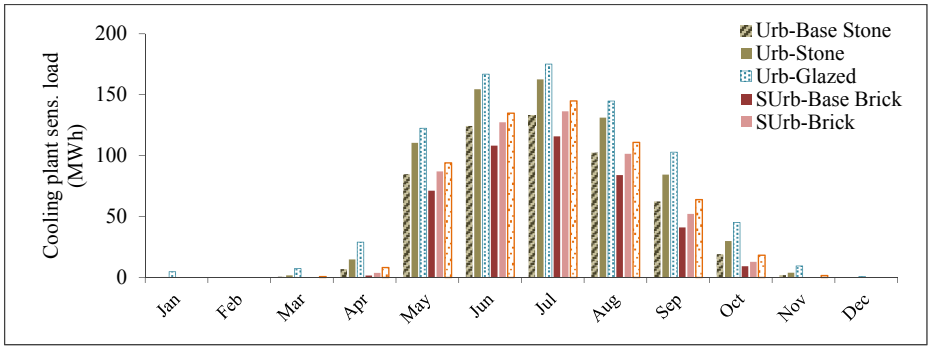

Fig. 12. Cooling plant sensible load monthly totals for scenarios (MWh).

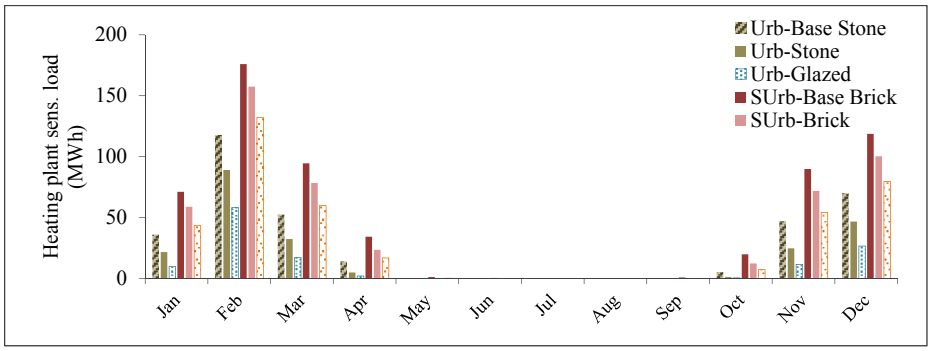

Fig. 13. Heating plant sensible load monthly totals for scenarios (MWh).

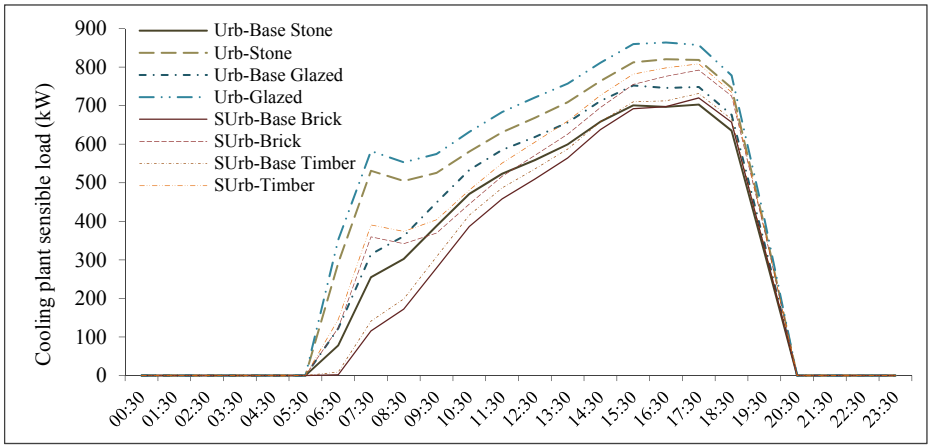

Fig. 14. Summer solstice (21-June) cooling load profiles for scenarios (kW).

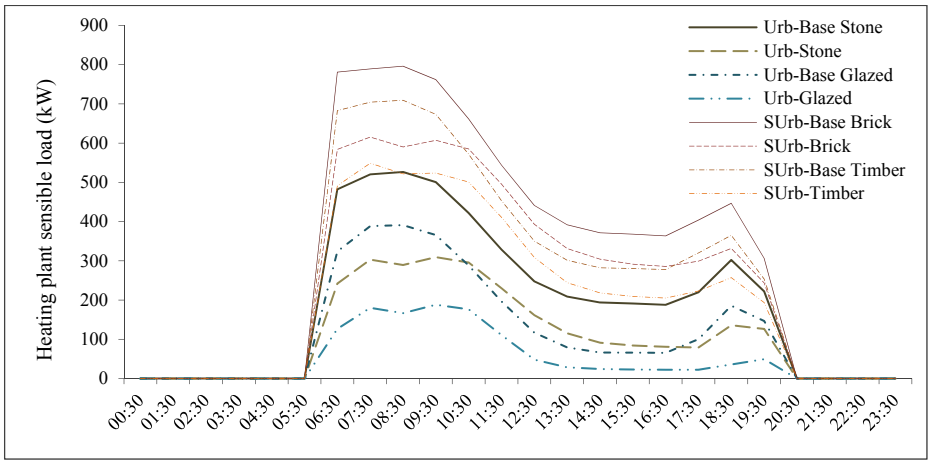

Fig. 15. Winter solstice (21-December) heating load profiles for scenarios (kW).

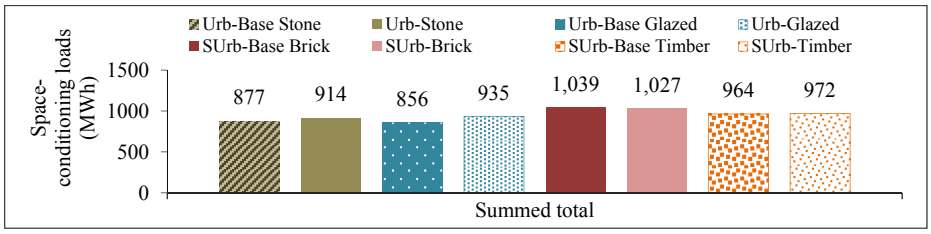

Fig. 16. Space-conditioning load comparison between Base and UHI influence included, for Urb-Stone and Urb-Glazed, and SUrb-Brick and SUrb-Timber facade (all with GR: 0.30) scenarios.

Including UHI influence on summer cooling and winter heating load values (see Fig. 12 to Fig. 16) demonstrated significant differences between urban and suburban scenarios. As the morphology of the suburban neighbourhood differs relative to its canyon (see Fig. 5 and Table 2), an east-facing and a west-facing unit was simulated to address any influence resulting from orientation. However, the space-conditioning results showed the difference between the two to be negligible, with west-facing totals <0.2 % (or <2 MWh) lower than the east-facing unit. Consequently for the rest of the study, the suburban condition is presented and discussed only in relation to the west-facing unit's simulations, which is consistent with the same presented for the urban simulations.

For the urban Stone scenario relative to its Base Stone simulation, including the UHI influence resulted in a 30 % increase in summertime cooling demand, while winter heating demand was reduced by 36 %. Overall, this meant that the influence of the UHI had an adverse effect on the space-conditioning demand of around 37 MWh, or a 4 % increased demand. When the urban Glazed scenario was compared against its Base Glazed simulation, UHI influence showed a 26 % increase in cooling demand and a 41 % decrease in heating demand. Overall, this meant that UHI influence had an adverse effect on the space-conditioning demand of around 82 MWh or a 10 % increased demand for the urban office building.

For the suburban Brick scenario relative to its Base Brick simulation, UHI influence resulted in a 21 % increase in summer cooling demand, while winter heating demand was reduced by 17 %. Overall, this meant that the UHI influence had a beneficial effect on its space-conditioning demand of around 13 MWh, or a 1.2 % decrease. When the suburban Timber scenario was compared against its Base Timber simulation, UHI influence showed a 21.2 % increase in cooling demand and a 19 % decrease in heating demand. Overall, this meant that UHI influence had a marginal adverse effect on its space-conditioning demand of around 8 MWh or a 0.8 % increased demand for the suburban office building.

The effect of transforming heavyweight to lightweight facades addressed by the urban comparison between Stone and Glazed scenarios (both with GR: 0.30 and UHI included), showed that the net annual space-conditioning demand increased by around 21 MWh or 2.3 % for the urban office building (relative heating load reduced by 43 %, and cooling load increased by 17 %). The corresponding suburban Brick to Timber comparison showed that the net annual space-conditioning demand decreased by around 54 MWh or 5 % for the suburban office building (relative heating load reduced by 22 %, and cooling load increased by 10 %, see Fig. 16).

4 Discussion

Historical observations of the London UHI reveals a diverse representation. The earliest observations of Howard [2] noted that London was 0.6 K warmer in the summer month of July and 1.2 K warmer in the winter month of November than the country. Howard [2] also observed that at night it was 2.05 K warmer, while during the day it was 0.19 K cooler. Chandler [19] examined temperature data for the period from 1931 to 1960 and found the annual mean to be 1.4 K warmer for central London, with 0.9 K warmer daytime maximum temperatures, and a monthly mean value of 1.6 K for the summer and 1.2 K for the winter. More recently, Watkins, Palmer [20] presented observational data from 1999 to show a summertime (June to August) excess of 2.8 K, and a peak value of 8 K. Data from 1999 also demonstrated a maximum summer daytime UHI of 8.9 K, while a nocturnal maximum of 8.6 K was observed during clear-sky periods with low (<5 ms^{-1}) wind velocity [21]. In winter, their data showed that the maximum UHI was 9 K both day and night under similar wind conditions [22]. In a recent study of west London urban parks, Doick, Peace [23] observed summertime nocturnal UHI peaks as high as 10 K on certain nights. A significant factor affecting the intensity of the UHI experienced is the radial distance from its urban core [24]. Watkins, Palmer [20] found that 77 % of the variance of the average night-time temperature across London strongly correlated to the radial distance of each location, although for the daytime the data presented a weaker 25 % variance.

Considering the above historic values, the UHIs simulated by the UWG could be said to fall within a plausible range, with the summertime average for the street canyons ranging between 1.85 to 1.86 K for Glazed and Stone urban scenarios, and 1.73 to 1.74 for Timber and Brick suburban scenarios respectively (see Fig. 6). The suburban conditions generate a relatively milder heat island to be experienced in the street canyon, which is illustrated clearly by the summer solstice profiles (see Fig. 8). This urban to suburban difference is therefore consistent with previous observations that suggest a decrease in heat island intensity when moving away from the city centre [20], which is generally an indication of morphological expansion (decreasing density or sprawl), and its associated changes in construction types and materiality.

When the summertime UHI averages for the canyons were separated into daytime and night-time averages, the lower averages for the daytime relative to the night-time simulated across the scenarios is consistent with most studies that highlight the peak UHI influence as a nocturnal occurrence [3, 25]. However, Howard's [2] finding of 0.19 K cooler daytime (i.e. cool island) London temperatures relative to the country was not predicted by any of the simulations. In general, the occurrence of cool island conditions with the urban scenarios in particular were less than expected, and limited to hourly occurrences as noted in the results above. This may be attributed to the 20 m street width being wide enough to minimise the canyon shading effect, and the notably higher anthropogenic heat output used for the Moorgate area (based on data from Iamarino, Beevers [26] simulations) contributing to relatively higher daytime canyon temperatures. The suburban scenarios in contrast present relatively cooler daytime temperatures, and a higher number of hours presenting cool island conditions to be experienced in the canyon. This may be attributed to the relatively lower anthropogenic heat

output from the suburban context and increased vegetation coverage contributing to a higher proportion of the ground surface flux being converted to latent flux.

The urban Stone scenario presented higher average UHI values relative to the Glazed scenario for the night-time, while the converse was true for the daytime. Similarly with the suburban scenarios, Brick presented higher (although marginally) values relative to Timber for the night-time, while the converse was true for the daytime. This suggests that fabrics with dominant heavyweight constructions such as stone at Moorgate, or brick at Wimbledon, could generate a warmer heat island effect to be experienced in their street canyons (particularly at night) relative to corresponding lightweight variations. When hourly resolution data was reviewed, the urban Stone scenario showed the highest number of hours reaching UHI ΔT maximum values. However for the suburban scenarios, these maximum UHI ΔT frequencies were similar for both. In terms of UHI ΔT minimum values, the urban Stone and suburban Brick scenarios showed the highest number of hours reaching these values predominantly during the daytime. This indicates that even though these material profiles have the potential to generate a warmer canyon temperature profile in the night-time, during the daytime they also have the potential to contribute to the greater experience of cool island conditions. This observation may be explained in relation to the thermal buffering properties offered by heavyweight materials such as stone and brick.

The materiality of urban form influences the surface energy balance by affecting both net radiation and heat storage. The radiative properties of materials are considered as emissivity and albedo, while storage properties are affected by heat capacity and thermal conductivity. The radiative property of albedo (α) or solar reflectance is defined as the percentage of solar energy reflected by a surface, and is a significant determinant of material surface temperatures [3, 27, 28]. Since 43 % of solar energy is in the visible wavelengths (400 to 700 nm), material colour is strongly correlated with albedo, with lighter coloured surfaces having higher values (α ~0.7) than darker surfaces (α ~0.2) [29]. For the urban condition, the stone was assumed to be Portland (typical for the Moorgate area), which is of a lighter colour and relatively high mean albedo of 0.6 [30]. With the suburban condition, the Timber was painted white to present an even higher albedo of 0.8. These albedos in turn contribute to lower radiation absorption by the facade material that helps to reduce their surface temperatures. As the summer (see Fig. 10) and winter (see Fig. 11) solstice surface temperature profiles for external walls demonstrate, during the midday period the temperature is lower for urban Stone surfaces compared to Glazed, and similarly the suburban Timber is lower relative to Brick. Furthermore this difference is pronounced during the summer when solar radiation influence is at its greatest. Such surface temperature differences between heavyweight and lightweight constructions can affect the urban microclimate both directly and indirectly. The direct effect is experienced in the form of its influence on reducing canyon ambient temperatures as cooler surfaces would have relatively lower sensible flux. The indirect effect works in conjunction with material heat storage properties to modify building energy use and its eventual feedback to the external microclimate.

Higher degrees of radiation reflection from high albedo materials mean that less energy is available for transfer into their depth. From the residual energy that is absorbed, a material's ability to store heat (capacity), which at times is referred to as thermal mass,

and thermal diffusivity, the ease by which heat penetrates into a material (function of thermal conductivity and volumetric heat capacity), determines its thermal inertia, a measure of the responsiveness of a material to temperature variations. Heavyweight materials such as stone and brick have relatively higher diffusivity, heat capacity, and thermal inertia, which means that their temperature fluctuations through the diurnal cycle are minimised [31]. Thus when radiation energy is received by such surfaces, the non-reflected energy is mostly absorbed and stored and when the climate above is relatively cooler, is re-radiated (as longwave) or purged back to the climate. This lag is evident when examining external surface temperature profiles (see Fig. 10 and Fig. 11), which show a lower daily variability range (amplitude) and delay in peak (phase shift) for urban Stone surfaces relative to Glazed surfaces. With the suburban profiles, the daily variability range (amplitude) is less pronounced than the urban comparison, and notably a delay or phase shift is not evident. This latter aspect means that the suburban scenarios seem to have greater relatability with the external microclimate relative to urban conditions, which is also a reflection of its reduced capacity to store heat.

From a building performance perspective, the material of the envelope absorbing more heat and storing it means that less thermal energy makes its way into the internal environments. This in turn helps to reduce their cooling loads and resulting heat rejection feedback to the climate, which is particularly evident in the daytime. This heat storage benefit of a heavyweight facade however can have a negative effect in the winter, as a significant proportion of the initial energy expenditure may be used to heat the facade rather than the internal environment. Lightweight constructions on the other hand demonstrate faster response to microclimate thermal changes, which explains their reduced demand in winter heating loads (see Fig. 13 and Fig. 15). Including the higher thermal load from the UHI therefore transfers readily into the internal spaces of the building to present a significant ‘winter warming effect’ (40 % and 19 % reductions for urban Glazed and suburban Timber scenarios respectively).

Materiality of urban built form can influence both the properties of the UHI as well as its impact on the building performance of this built form. The properties of the dominant material profile in an urban setting is identified in previous research to modify the intensity and timing of when the UHI peak is likely to be observed [3]. Cities made of predominantly higher diffusivity materials such as stone are unlikely to reach their UHI peak until sunrise, while those made of lower diffusivity materials are suggested to reach their peak soon after sunset [31]. This study demonstrates this to be true for the urban Stone and suburban Brick scenarios with the peak evident towards sunrise. However, both the urban Glazed and suburban Timber scenarios do not demonstrate the phase shift to confirm the latter observation for lightweight constructions (see Fig. 7 and Fig. 8). Conversely, the thermal efficiencies of the building envelope have a significant influence on the degree of benefit or detriment that the UHI load presents to their space-conditioning loads. In this study, the space-conditioning loads demonstrated that Stone and Brick constructions could be said to accommodate the additional thermal load from the UHI relatively better over the course of the year than lightweight Glazed or Timber constructions of the same GR.

5 Summary

In any form of development that takes place in a city, the construction materials used and their properties of emissivity, albedo, heat capacity, and thermal conductivity determine how solar energy is reflected, emitted, and absorbed by surfaces. The properties of the dominant material within this setting may affect the intensity and the timing of when the UHI peak is likely to be observed, and how the UHI load itself is transferred into internal environments to affect space-conditioning performance. It is worth noting that materiality is an aspect of existing built form that can be reasonably modified, perhaps to a greater degree of practicability than its morphology. Tasks of regenerating urban and suburban areas therefore have the opportunity to reconsider material choices in light of how they affect the urban energy balance, and in turn offer greater potential for heat mitigation and reduced building energy use.

This study has shown that the trend in urban centres to construct highly glazed buildings with lightweight insulated facades increases space-conditioning loads and adversely affects the UHI, thereby creating a vicious cycle of additional urban heating that exacerbates the impacts of climate change. Within a suburban context however, changing from heavyweight to lightweight insulated facades decreased space-conditioning loads to provide a beneficial effect. The study in turn stresses the significance of accounting for UHI loads in estimating urban energy use, for which a combined simulation approach of using an urban climate model and a building energy model has been presented as a feasible pathway.

6 Appendix

Table 2. Parameters used for simulations.

	Parameter	Moorgate (central urban)	Wimbledon (suburban)
Block	Canyon block dimensions	L 60 × D 35 × H 24.5 m	L 60 × D 35 × H 24.5 m
	Context block dimensions	L 60 × D 35 × H 24.5 m	L 60 × D 35 × H 10.5 m
	Average floor height	3.5 m	3.5 m
	Assumed building use	Medium office	Medium office
	Total office area in radius	3,410,400 m^2	2,360,400 m^2
Simplified Base (*existing heavy-weight*) constructions	Wall material and thickness	***STONE:*** Portland stone/plaster Thickness: 0.3/0.025 m U-value: 2.33 W m^{-2} K^{-1}	***BRICK:*** Brick/gypsum plaster Thickness: 0.215/0.035 m U-value: 1.96 W m^{-2} K^{-1}
	Roof material and thickness	Type: Flat roof Gravel/expanded polystyrene/concrete/ceiling tiles Thickness: 0.075/0.1/0.3/0.05 m U-value: 0.24 W m^{-2} K^{-1}	Type: Inclined roof (45°) Clay tiled/timber insulation/gypsum plasterboard Thickness: 0.015/0.1/0.25/0.015 m U-value: 0.23 W m^{-2} K^{-1}
	Glazing	GR: 0.3 (30 %) U-value: 1.93 W m^{-2} K^{-1}	GR: 0.3 (30 %) U-value: 1.93 W m^{-2} K^{-1}

	Parameter	Moorgate (central urban)	Wimbledon (suburban)
	Initial temperature of construction	20 ˚C	20 ˚C
	Gains: lighting and equipment	12 and 25 W m^{-2}	12 and 25 W m^{-2}
	Gains: Occupancy	6 m^2 $person^{-1}$	6 m^2 $person^{-1}$
	Gains profile used	@ medium office schedule †	@ medium office schedule
	Infiltration	0.5 ach	0.5 ach
	Ventilation	0.002 m^3 s^{-1} m^{-2}	0.002 m^3 s^{-1} m^{-2}
	Cooling system	Air	Air
	Heating efficiency	0.80	0.80
	Daytime and night-time set points	@ medium office schedule	@ medium office schedule
	Heat rejected to canyon	50%	25%
Roads	Material and Thickness	Asphalt / 0.5 m	Asphalt / 0.5 m
Urban & Rural	Vegetation coverage ratio	Urban: 0.005 Rural: 0.8	0.2 0.8
Urban area	***Average building height****	***24.5 m***	***10.8 m***
	Horizontal building density ratio*	***0.598***	***0.480***
	Vertical to horizontal area ratio*	***0.99***	***0.35***
	Tree coverage ratio	0.001	0.080
	Non-building sensible heat rejection	22.68 W m^{-2}	1.77 W m^{-2}
	Non-building latent heat rejection	2.268 W m^{-2}	0.18 W m^{-2}
	Characteristic neighbourhood length	500 m	500 m
	Tree and grass latent fractions	0.7 and 0.5	0.7 and 0.5
	Vegetation albedo	0.25	0.25
	Vegetation contribution start-end	April to October	April to October
	Daytime boundary layer height	1000 m	850 m
	Night-time boundary layer height	80 m	50 m
Reference site	Latitude, longitude (for *Reading*)	51.446, - 0.957	51.446, - 0.957
	Distance from study sites	~60 km due west	~52 km due west

* Key neighbourhood morphological parameters.

† Medium office schedule: Weekdays from 7 AM to 7 PM (at 0.9 load); Saturday from 7 AM to 5 PM (at 0.4 load); and Sunday full-day (at 0.1 load).

Table 3. Construction parameters changed for lightweight material simulations

	Parameter	Moorgate (central urban)	Wimbledon (suburban)
Simplified (*hypothetical lightweight*) constructions	Wall material and thickness	***GLAZED:*** Anti-sun glass cladding/expanded polystyrene/gypsum plasterboard Thickness: 0.010/0.1/0.025 m U-value: 0.31 W m^{-2} K^{-1}	***TIMBER:*** White painted sheathing/expanded polystyrene/timber frame/gypsum plasterboard Thickness: 0.02/0.1/0.025/0.025 m U-value: 0.28 W m^{-2} K^{-1}

References

1. UN, *World Urbanization Prospects: Highlights*. 2014, United Nations: New York.

2. Howard, L., *The climate of London : deduced from meteorological observations made in the metropolis and at various places around it*. 1833, London: Harvey and Darton, J. and A. Arch, Longman, Hatchard, S. Highley [and] R. Hunter.

3. Oke, T.R., *Boundary Layer Climates*. 2 ed. 1987, New York: Routledge.

4. Oke, T.R., *The Energetic Basis of the Urban Heat-Island.* Quarterly Journal of the Royal Meteorological Society, 1982. **108**(455): p. 1-24.

5. Grimmond, C., et al., *Climate and more sustainable cities: climate information for improved planning and management of cities (producers/capabilities perspective).* Procedia Environmental Sciences, 2010. **1**: p. 247-274.

6. Pigeon, G., et al., *Urban thermodynamic island in a coastal city analysed from an optimized surface network.* Boundary-Layer Meteorology, 2006. **120**(2): p. 315-351.

7. Kolokotroni, M., Y.P. Zhang, and R. Watkins, *The London Heat Island and building cooling design.* Solar Energy, 2007. **81**(1): p. 102-110.

8. Hidalgo, J., G. Pigeon, and V. Masson, *Urban-breeze circulation during the CAPITOUL experiment: observational data analysis approach.* Meteorology and Atmospheric Physics, 2008. **102**(3-4): p. 223-241.

9. Oxizidis, S., A. Dudek, and A. Papadopoulos, *A computational method to assess the impact of urban climate on buildings using modeled climatic data.* Energy and Buildings, 2008. **40**(3): p. 215-223.

10. Bueno, B., et al., *The urban weather generator.* Journal of Building Performance Simulation, 2013. **6**(4): p. 269-281.

11. Norford, L., et al., *Urban Weather Generator*. 2017, University of Bath: Bath.

12. Norford, L., et al., *Urban Weather Generator*. 2015, Building Technology Program, Massachusetts Institute of Technology: Cambridge, Massachusetts.

13. Masson, V., *A physically-based scheme for the urban energy budget in atmospheric models.* Boundary-layer meteorology, 2000. **94**(3): p. 357-397.

14. Bueno, B., et al., *A resistance-capacitance network model for the analysis of the interactions between the energy performance of buildings and the urban climate.* Building and Environment, 2012. **54**: p. 116-125.

15. Bueno, B., et al., *Computationally efficient prediction of canopy level urban air temperature at the neighbourhood scale.* Urban Climate, 2014. **9**: p. 35-53.

16. Nakano, A., et al., *Urban Weather Generator - A novel workflow for integrating urban heat island effect within urban design process*, in *Building Simulation 2015*. 2015, International Building Performance Simulation Association: Hyderabad, India.

17. Eames, M., T. Kershaw, and D. Coley, *On the creation of future probabilistic design weather years from UKCP09.* Building Services Engineering Research & Technology, 2011. **32**(2): p. 127-142.

18. IES-VE, *IES-Virtual Environment 2015*. 2015, Integrated Environmental Solutions Ltd: Glasgow.

19. Chandler, T.J., *The Climate of London*. 1965, London: Hutchinson & Co Ltd.

20. Watkins, R., et al., *The London Heat Island: results from summertime monitoring.* Building Serv. Eng. Res. Technol. , 2002. **23**(2): p. 97-106.

21. Kolokotroni, M. and R. Giridharan, *Urban heat island intensity in London: An investigation of the impact of physical characteristics on changes in outdoor air temperature during summer.* Solar Energy, 2008. **82**(11): p. 986-998.

22. Giridharan, R. and M. Kolokotroni, *Urban heat island characteristics in London during winter.* Solar Energy, 2009. **83**(9): p. 1668-1682.

23. Doick, K.J., A. Peace, and T.R. Hutchings, *The role of one large greenspace in mitigating London's nocturnal urban heat island.* Sci Total Environ, 2014. **493**: p. 662-71.

24. Kolokotroni, M., Y. Zhang, and R. Giridharan, *Heating and cooling degree day prediction within the London urban heat island area.* Building Services Engineering Research and Technology, 2009. **30**(3): p. 183-202.

25. Wilby, R.L., *Past and projected trends in London's urban heat island.* Weather, 2003. **58**.

26. Iamarino, M., S. Beevers, and C.S.B. Grimmond, *High-resolution (space, time) anthropogenic heat emissions: London 1970-2025.* International Journal of Climatology, 2012. **32**(11): p. 1754-1767.

27. Taha, H., *Urban climates and heat islands: Albedo, evapotranspiration, and anthropogenic heat.* Energy and Buildings, 1997. **25**(2): p. 99-103.

28. Jacobson, M.Z., *Fundamentals of atmospheric modeling*. 2005, Cambridge: Cambridge University Press.

29. Taha, H., et al., *Residential Cooling Loads and the Urban Heat-Island - the Effects of Albedo.* Building and Environment, 1988. **23**(4): p. 271-283.

30. Yates, T., *Jordans basebed technical data sheet*, in *Building Research Establishment (BRE)*. 2017, Building Research Establishment (BRE) on behalf of Albion Stone: Surrey.

31. Gartland, L., *Heat Islands: Understanding and Mitigating Heat in Urban Areas*. 2008, Oxford: Routledge.